

- 19 Stack, J. H., Horazdovsky, B. and Emr, S. D. (1995) *Annu. Rev. Cell Dev. Biol.* 11, 1–33
- 20 Babst, M. *et al.* (1997) *EMBO J.* 16, 1820–1831
- 21 Cowles, C. R. *et al.* (1997) *EMBO J.* 16, 2769–2782
- 22 Piper, R. C., Bryant, N. J. and Stevens, T. H. (1997) *J. Cell Biol.* 138, 531–545
- 23 Raymond, C. K. *et al.* (1992) *Mol. Biol. Cell* 3, 1389–1402
- 24 Nothwehr, S. F., Conibear, E. and Stevens, T. H. (1995) *J. Cell Biol.* 129, 35–46
- 25 Herman, P. K., Stack, J. H. and Emr, S. D. (1991) *EMBO J.* 10, 4049–4060
- 26 Stack, J. H. *et al.* (1995) *J. Cell Biol.* 129, 321–334
- 27 Horazdovsky, B. F. *et al.* (1996) *J. Biol. Chem.* 271, 33607–33615
- 28 Cowles, C. R. *et al.* (1997) *Cell* 91, 109–118
- 29 Stepp, J. D., Huang, K. and Lemmon, S. K. (1997) *J. Cell Biol.* 139, 1761–1774
- 30 Novick, P. and Schekman, R. (1979) *Proc. Natl. Acad. Sci. U. S. A.* 76, 1858–1862
- 31 Cowles, C. R., Emr, S. D. and Horazdovsky, B. F. (1994) *J. Cell Sci.* 107, 3449–3459
- 32 Darsow, T., Rieder, S. E. and Emr, S. D. (1997) *J. Cell Biol.* 138, 517–529
- 33 Ooi, C. E. *et al.* (1997) *EMBO J.* 16, 4508–4518
- 34 Lloyd, V., Ramaswami, M. and Krämer, H. (1998) *Trends Cell Biol.* 8, 257–259
- 35 Morgan, T. H. (1910) *Science* 32, 120–122
- 36 Shestopal, S. A. *et al.* (1997) *Mol. Gen. Genet.* 253, 642–648
- 37 Rieder, S. E. and Emr, S. D. (1997) *Mol. Biol. Cell* 8, 2307–2327
- 38 Nakamura, N. *et al.* (1997) *J. Biol. Chem.* 272, 11344–11349
- 39 Radisky, D. C. *et al.* (1997) *Proc. Natl. Acad. Sci. U. S. A.* 94, 5662–5666
- 40 Banta, L. M. *et al.* (1988) *J. Cell Biol.* 107, 1369–1383
- 41 Nickla, H. (1977) *Nature* 268, 638–639
- 42 Keeler, C. (1978) in *Origins of Inbred Mice* (Morse, H. C., ed.), pp. 179–192, Academic Press
- 43 Orlow, S. J. (1995) *J. Invest. Dermatol.* 105, 3–7
- 44 Jackson, I. J. (1994) *Annu. Rev. Genet.* 28, 189–217
- 45 Barbosa, M. D. *et al.* (1996) *Nature* 382, 262–265
- 46 Perou, C. M. *et al.* (1996) *Nat. Genet.* 13, 303–308
- 47 Gardner, J. M. *et al.* (1997) *Proc. Natl. Acad. Sci. U. S. A.* 94, 9238–9243
- 48 Feng, G. H. *et al.* (1997) *Hum. Mol. Genet.* 6, 793–797
- 49 Jimbow, K. *et al.* (1997) *Pigment Cell Res.* 10, 206–213
- 50 Winder, A. J. *et al.* (1993) *J. Cell Sci.* 106, 153–166
- 51 Vijayaradhi, S. *et al.* (1995) *J. Cell Biol.* 130, 807–820
- 52 Beermann, F. *et al.* (1995) *Exp. Eye Res.* 61, 599–607
- 53 Kwon, B. S. *et al.* (1995) *Nucleic Acids Res.* 23, 154–158
- 54 Honing, S., Sandoval, I. V. and von Figura, K. (1998) *EMBO J.* 17, 1304–1314
- 55 Sandoval, I. V. and Bakke, O. (1994) *Trends Cell Biol.* 4, 292–297
- 56 Vowels, J. J. and Payne, G. S. (1998) *EMBO J.* 17, 2482–2493
- 57 Kornfeld, S. and Mellman, I. (1989) *Annu. Rev. Cell Biol.* 5, 483–525
- 58 Brodsky, F. M. (1997) *Trends Cell Biol.* 7, 175–179
- 59 Faúndez, V., Horng, J.-T. and Kelly, R. B. (1998) *Cell* 93, 423–432
- 60 Lane, P. W. and Deol, M. S. (1974) *J. Hered.* 65, 362–364
- 61 Peters, P. J. *et al.* (1991) *Nature* 349, 669–676
- 62 Robinson, M. S. (1997) *Trends Cell Biol.* 7, 99–102

## Acknowledgements

The authors thank Greg Payne, Scottie Robinson, Richard Swank, Margit Burmeister, Barbara Wakimoto, Bernard Hoflack, Regis Kelly and Juan Bonifacino for many helpful discussions and for communicating unpublished data.

## Digital imaging microscopy of living cells

Rosario Rizzuto, Walter Carrington and Richard A. Tuft

*Fluorescence microscopy has undergone a resurgence in interest following the discovery of green-fluorescent protein (GFP) and its increasing use in live-cell imaging. This article describes an enhanced form of epifluorescence microscopy, digital imaging microscopy, that can be used to produce high-resolution three-dimensional images of samples labelled with GFP, or other fluorochromes, using simple instrumentation and image-restoration software.*

Much of the recent progress in understanding the biology of individual cells has come through study of the structural organization of the key components of signalling and regulatory pathways. Central to this understanding has been the ability to image, visualize and analyse the cell

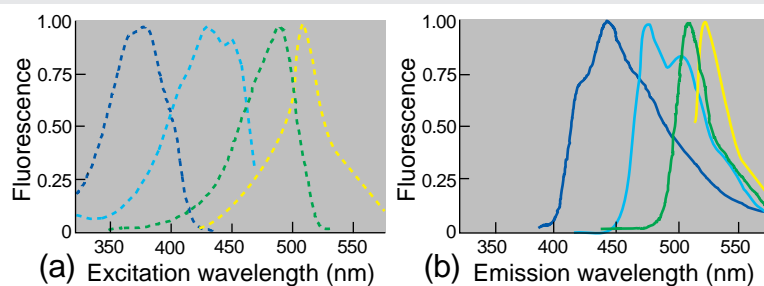
as a three-dimensional (3-D) object. A single image taken with a standard epifluorescence microscope produces a 2-D representation of a complex 3-D specimen. Small features adjacent to each other in the plane-of-focus (X–Y) can be resolved distinctly, but the contrast between

them is reduced by out-of-focus fluorescence from the remainder of the cell, and their spatial relationship to each other might therefore be obscured. The spatial relationship of features separated in the focus (or Z) direction is often not apparent at all. The reduced contrast and the lack of a fully connected 3-D view in a conventional fluorescence microscope hinder understanding of the organization of the fluorescent probe throughout the volume of the cell.

In this article, we describe an approach, known as the digital imaging microscope (DIM), which uses sequentially focused wide-field fluorescence images and computational algorithms to reconstruct high-resolution 3-D images. Because it involves imaging in parallel, wide-field microscopy requires a weaker illumination intensity than confocal microscopy, and, with appropriately designed filters, all green-fluorescent protein (GFP; see Box 1) mutants can be employed, alone or in combination. Moreover, computation allows a significant improvement in spatial

**BOX 1—GREEN FLUORESCENT PROTEIN**

The green-fluorescent protein (GFP) of *Aequorea victoria* has emerged as a unique new tool with exciting applications in cell biology<sup>1-3</sup>. Its properties make it an ideal fluorescent probe: its fluorescence is not species specific (its simple recombinant expression yields a strong fluorescence signal in cell systems as diverse as bacteria, yeasts, plants and mammalian cells), no cofactor is needed, and the protein is relatively small (238 amino acids), allowing fusion to proteins of interest without interfering significantly with their assembly or function. Following the first report of the recombinant expression of GFP<sup>1</sup>, interest in this protein has grown rapidly; GFP is now a widely employed reporter for a variety of cellular phenomena and it is likely that GFP applications will continue to increase. A number of mutants are now available with increased fluorescent emission<sup>4,5</sup> and with their excitation or emission spectra shifted from that of wild-type GFP<sup>6-9</sup> (see figure), which both enhances their efficiency as reporter proteins and allows simultaneous *in vivo* labelling of two or more proteins, compartments or cell lineages of interest<sup>10</sup>. Moreover, fluorescence resonance energy transfer (FRET) between GFP mutants opens the way to novel approaches for dynamically monitoring protein-protein interactions, as well as other physiological events, in living cells. In fact, it has been recently demonstrated that FRET between two GFP mutants connected via a Ca<sup>2+</sup>-sensitive linker is a function of [Ca<sup>2+</sup>], and that this chimera can be employed *in vivo* as a recombinant Ca<sup>2+</sup> probe<sup>11,12</sup>. These probes might represent the first examples of novel indicators for key cellular parameters or events (ion concentration, phosphorylation, etc.) and can be expressed easily in virtually every cell type and targeted to the cell region of interest, further expanding the potential applications of GFP in cell biology.



The wavelength-shifted mutants of GFP. The left and right panels show, respectively, the excitation and emission spectra of the Y66H (blue line), Y66W (turquoise line), S65T,A,C (green line) and T203Y (yellow line) mutants.

resolution (to ~100 nm, several times higher than with traditional confocal or epifluorescence microscopy). Here, we describe the use of a single targeted GFP probe as the experimental example. However, this imaging approach can be applied successfully to all the various GFP moieties and chimeras as well as to standard fluorescent probes. Moreover, with a filter wheel alternating the excitation wavelength, simultaneous imaging of

probes based on different GFP mutants can be attained easily.

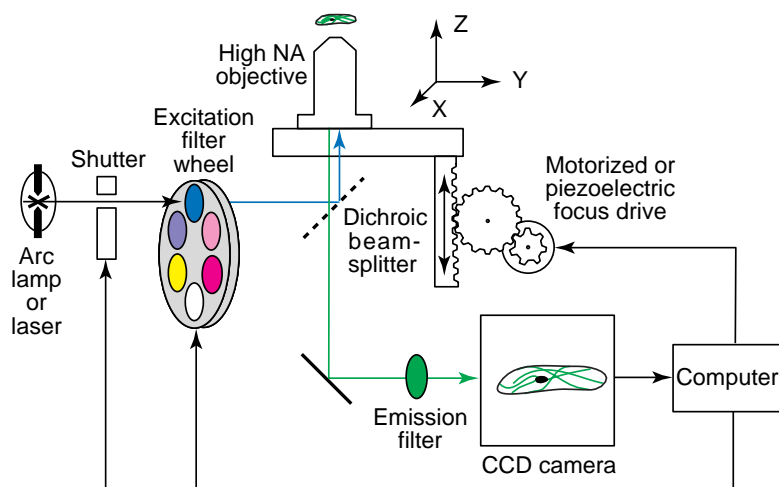
**Basic acquisition system and operating principles**

Figure 1 presents a diagram of the essential elements of a DIM. It can usually be built using any of the modern commercial wide-field epifluorescence microscopes, either upright or inverted. In addition to a standard arc lamp illuminator (generally Hg or Xe, or both),

a DIM requires a high-resolution focus drive and a scientific charge coupled device (CCD) camera. The focus drive can be either a motor or a piezoelectric translator. The CCD camera is one of the most important components because its quantum efficiency (QE) and readout noise are crucial determinants of system performance. For the most crucial imaging applications, such as the multiple-exposure imaging of living cells, we find that thinned, back-illuminated CCDs with ~70% QE and readout noise of <10 electrons per picture element (pixel) give good results. A computer-controlled filter wheel facilitates the use of several wavelength-shifted GFP chimeras in one experiment by allowing rapid alteration of the excitation wavelength. Under computer control, the instrument takes exposures, or optical sections, at sequential focal planes within the cell. The images in this data set are then computer processed using an image-restoration algorithm to produce a 3-D image of the cell, which can be displayed and viewed as a volume, from any angle, on a computer monitor. Over 1600 optical sections, producing 40 3-D images, have been obtained from a single GFP-labelled cell by using such a system.

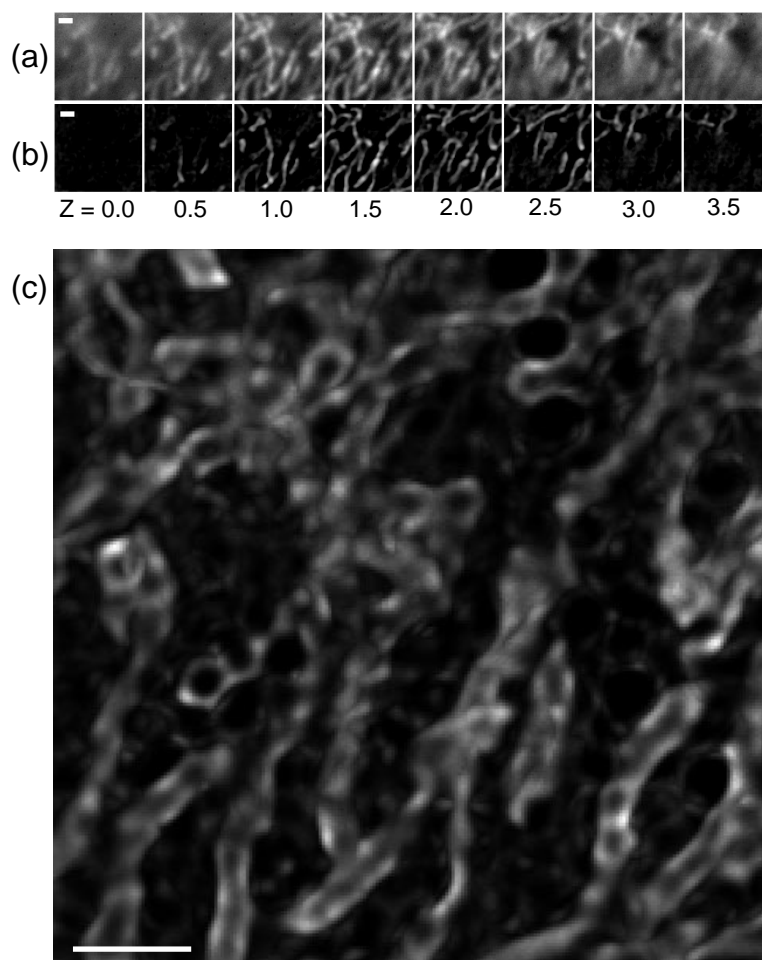
**Image restoration**

Image restoration, also known as deconvolution or computational

**FIGURE 1**

Essential components of a digital imaging microscope (DIM). These systems can be built on any of today's excellent epifluorescence microscopes. A number of vendors sell the integrated add-on hardware and software to control the instrument and perform image restoration and image display (see Table 1).

Rosario Rizzuto is in the Dept of Biomedical Sciences and CNR Center for the Study of Biomembranes, University of Padova, Via Colombo 3, 37121 Padova, Italy; and Walter Carrington and Richard Tuft are in the Biomedical Imaging Group, University of Massachusetts Medical Center, 373 Plantation Street, Worcester, MA 01605, USA. E-mail: rizzuto@civ.bio.unipd.it



**FIGURE 2**

Three-dimensional (3-D) image of mitochondria in a live cell, labelled with a specifically targeted green-fluorescent protein chimera (mtGFP)<sup>22</sup>. Bars, 1  $\mu\text{m}$ . (a) Set of optical sections of GFP fluorescence before processing. The objective lens used was a 100 $\times$  NA 1.4 Planapo. The pixel size is 80 nm, and the spacing between the sections shown is 500 nm. The full data set consists of 21 optical sections at 250 nm, spaced from the top of the cell to the bottom. Note the substantial amount of out-of-focus light present as haze in the images. The data were collected on a custom-designed digital imaging microscope (DIM,) with wide-field 488-nm laser illumination and an experimental high-speed charge coupled device (CCD) camera. Optical sections were acquired with 20 msec exposure, with 10 msec between sections to shift focus. (b) Image restoration of the data in (a). The same pixel size and step size in the focus direction (z) were used in the calculations as in the data; all 21 optical sections at 250-nm spacing were used. Note that the out-of-focus light is substantially eliminated and resolution is increased. Image restoration was performed with software developed at UMASS Medical Center and licensed to Scanalytics, Inc. (c) 3-D projection of image restoration of data in (a) calculated on a finer grid. In this image restoration, the calculations were performed on a grid with 27-nm subpixels and 125-nm steps in Z (i.e. three times finer in the X-Y plane of focus and two times finer in Z than the sampling of the data). Software developed at UMASS Medical Center, not yet commercially available, was used for this restoration.

optical-sectioning microscopy, is a process that computes a high-resolution 3-D image of a cellular fluorescence distribution from three pieces of information:

- A 3-D image of the cell in the form of optical sections.
- A quantitative calibration of the spatial blurring of the microscope, generally in the form of a 3-D image

of a small fluorescent bead. This 'point spread function' (PSF) provides the information needed for a computer simulation of the 3-D imaging process.

- Constraints on the fluorescence distribution (e.g. fluorescence intensity must be non-negative). Image restoration generates a 3-D fluorescence image of the sample

that is quantitatively more accurate than the unprocessed data: out-of-focus haze is removed, the resolution and contrast are increased, and quantitative fluorescence measurements are more accurate than with the unprocessed data. Several computationally intensive nonlinear iterative algorithms have been applied successfully to 3-D fluorescence imaging<sup>15-19</sup>. Algorithms can be designed to produce a fluorescence estimate whose simulated data match the measured data as well as possible. However, this approach magnifies any noise present in the measured data. Therefore, the most successful algorithms impose some smoothing on the fluorescence density, either explicitly or implicitly. The approach we use minimizes noise and errors by an explicit smoothing based on an extensive mathematical theory<sup>18,20</sup>. Our approach also differs from others in its model of the imaging process – as it considers the cell as a continuous object. Image data, on the other hand, are composed of a finite number of discrete pixels. This discrete data/continuous cell model allows reconstruction of the cell on a grid that is finer than the sampling grid of the data.

### Example application

The biological sample analysed in Figure 2 shows a clear example of the increase in image quality and resolution that can be obtained with this computational method. In the unprocessed image, Figure 2a, the pixels are 80 nm square. Restoration of these data with the same pixel size is shown in Figure 2b. Figure 2c shows what can be achieved with our most recent algorithm. It shows an image computed from the same data with subpixels smaller by a factor of three in the X-Y plane and two in the Z plane. This result could also be obtained by using greater magnification and finer focus steps, but, since the light would be spread out over 18 times as many pixels, 18 times the light exposure would be required to obtain the same signal : noise ratio. This flexibility can also be used to reduce the number of optical sections needed for live-cell imaging, thus reducing the light exposure<sup>18,20,21</sup>.

Resolution using this sub-pixel approach has been tested in several ways. In cells, it is possible to resolve branching microtubules when the two branches are separated by 112 nm (Ref. 18). In a recent experiment in which a very accurate

**TABLE 1 – EQUIPMENT PROVIDERS**

	City	Web site
<b>CCD camera manufacturers</b>		
Photometrics	Tucson, Arizona 85706, USA	www.photomet.com
Princeton Instruments	Trenton, New Jersey 08619, USA	www.prinst.com
<b>Software and integrated system suppliers</b>		
Applied Precision	Issaquah, Washington, USA	www.api.com
AutoQuant Imaging	Watervliet, New York, USA	www.aqi.com
Improvision	Coventry, UK	www.improvision.com
Scanalytics	Fairfax, Virginia, USA	www.scanalytics.com
Scientific Volume Imaging	Hilversum, Netherlands	www.svi.nl
Universal Imaging	Westchester, Pennsylvania, USA	www.image1.com
Vaytek	Fairfield, Iowa, USA	www.vaytek.com

Abbreviation: CCD, charge coupled device.

piezoelectric driver was used to move a fluorescent bead of diameter 40 nm, bead images separated by 100 nm were fully resolved – the two bright spots were separated by a black zero-intensity region. This

resolution is several-fold better than that achieved by confocal or wide-field microscopy without image restoration. In addition, as can be seen in Figure 2a, the raw data contain a great deal of haze from out-

of-focus light. In the restored images, this haze has gone and contrast is much enhanced. The numerical accuracy of fluorescence quantification in the restored images is also much improved.

**BOX 2 – DIM AND CONFOCAL MICROSCOPY**

The digital imaging microscope (DIM) is one of several approaches developed over the past 15 years to deal with the three-dimensional nature of microscopic images and the problem of out-of-focus light (see Table 2). Laser scanning confocal microscopes<sup>13</sup> (LSCMs) optically reject out-of-focus light and provide instant viewing without image restoration, a computation that takes several minutes to many hours. LSCMs can also image simultaneously two (or more) emission wavelengths during a single image scan. In commercially available LSCMs, light losses in the scanning optics and the lower quantum efficiency of the photomultiplier detectors can result in LSCM collection efficiencies that are a factor of two to ten times lower than a DIM, leading to increased photobleaching. Furthermore, an LSCM image is created point by point as the laser beam is scanned throughout the sample volume and so can improperly reflect a cellular process that is changing rapidly compared with the time to scan the volume.

While both DIMs and LSCMs excite fluorescence throughout the whole depth of the sample at each plane of focus, the newer two-photon and multiple-photon LSCMs<sup>14</sup> excite a layer only one to several microns thick, considerably reducing photobleaching. The longer excitation wavelength of multiple-photon LSCMs also reduces photodamage. Both single and multiple-photon LSCMs provide superior contrast and resolution when imaging deep into thick specimens.

**TABLE 2 – PROS AND CONS OF IMAGING TECHNIQUES**

DIM	LSCM	Two-photon
<b>Advantages</b>		
Low cost	Instant viewing	Instant viewing
High acquisition speed	Analysis of thick samples	Analysis of thick samples
Reduced photobleaching and photodamage		Reduced photobleaching and photodamage
<b>Disadvantages</b>		
Requires accurate PSF	High photobleaching and photodamage	Limited number of excitation wavelengths
Heavy computation	Limited number of excitation wavelengths	High cost
Off-line analysis and viewing	Fluorescence saturation	Fluorescence saturation

Abbreviations: DIM, digital imaging microscope; LSCM, laser scanning confocal microscope; PSF, point spread function.

**Acknowledgements**

This article is dedicated to the memory of the late Fred Fay, an innovative scientist and a dear friend, who pioneered the approach described in this contribution. The experimental work was supported by funds from 'Telethon' (project n. 850), the 'Biomed' programme of the European Union, the Italian University Ministry, NATO and the British Research Council to R. R., and by grants from the National Science Foundation (DBI-9200027, DBI-9724611) and the NIH (HL14523, HL47530, RR09799-01A2) to W. C. and R. A. T.

**Guidelines for building a DIM system**

Table 1 lists some of the vendors of CCD cameras as well as the hardware and software that can be used to control the imaging hardware and perform image restorations. This list is not intended to be exhaustive and does not represent an endorsement of any given product. DIMs have been configured to perform cellular imaging over a range of time scales, resolutions and signal intensities. In all applications, the CCD camera is generally the most important component: a high QE, low-noise CCD will be the ultimate determinant of system sensitivity and resolution.

**Concluding remarks**

Digital imaging microscopy, in its most basic form, is a relatively inexpensive alternative to confocal microscopes (for a comparison of the two, see Box 2). Its use of wide-field microscopy and sensitive CCD cameras makes it particularly useful for repeated 3-D imaging of live single cells with GFP. Recent advances in image-restoration methods provide high-resolution 3-D images that show cellular detail not available from

other methods. Recently published studies demonstrate both the high spatial resolution to which this method can be extended<sup>23</sup>, as well as the quantitative accuracy that can be obtained with single-molecule probes labelled with as few as five fluorochromes<sup>24</sup>.

**References**

- 1 Chalfie, M. *et al.* (1994) *Science* 263, 802–805
- 2 Cubitt, A. B. *et al.* (1995) *Trends Biochem. Sci.* 20, 448–455
- 3 Sullivan, K. F. and Kay, S. A. *Methods Cell Biol.* (in press)
- 4 Heim, R., Cubitt, A. B. and Tsien, R. Y. (1995) *Nature* 373, 663–664
- 5 Cormack, B. P., Valdivia, R. H. and Falkow, S. (1996) *Gene* 173, 33–38
- 6 Heim, R., Prasher, D. and Tsien, R. Y. (1994) *Proc. Natl. Acad. Sci. U. S. A.* 91, 12501–12504
- 7 Heim, R. and Tsien, R. Y. (1996) *Curr. Biol.* 6, 178–182
- 8 Ehrig, T., O’Kane, D. J. and Prendergast, F. G. (1995) *FEBS Lett.* 367, 163–166
- 9 Levy, J. P. *et al.* (1996) *Nat. Biotechnol.* 14, 610–614
- 10 Rizzuto, R. *et al.* (1996) *Curr. Biol.* 6, 183–188
- 11 Miyawaki, A. *et al.* (1997) *Nature* 388, 882–887
- 12 Rosmoser, V. A., Hinkle, P. M. and Persechini, A. (1997) *J. Biol. Chem.* 272, 13270–13274
- 13 *Handbook of Biological Confocal Microscopy* (1995) (Pawley, J. B., ed.), Plenum Press
- 14 Denk, W., Strickler, J. H. and Webb, W. W. (1990) *Science* 248, 73–76
- 15 Agard, D. A. (1984) *Annu. Rev. Biophys. Bioeng.* 13, 191–219
- 16 Agard, D. A. *et al.* (1989) *Methods Cell Biol.* 30, 353–377
- 17 Carrington, W. A., Fogarty, K. E. and Fay, F. S. (1990) in *Non-invasive Techniques in Cell Biology* (Foster, K. and Grinstein, S., eds), pp. 53–72, Wiley-Liss
- 18 Carrington, W. A. *et al.* (1995) *Science* 268, 1483–1487
- 19 Conchello, J. A., Yu, Q. and Lichtman, J. W. (1994) *SPIE Proc.* 2302, 379–388
- 20 Carrington, W. A. (1990) *SPIE Proc.* 1205, 72–83
- 21 Lynch, R. M. *et al.* (1996) *Am. J. Physiol.* 270, C488–C499
- 22 Rizzuto, R. *et al.* (1995) *Curr. Biol.* 5, 635–642
- 23 Dichtenberg, J. B. *et al.* (1998) *J. Cell Biol.* 141, 163–174
- 24 Femino, A. M. *et al.* (1998) *Science* 280, 585–590

## Stuck on the ECM

Li-Huei Tsai

One of the Keystone meetings in early April\* consisted of two simultaneous conferences on extracellular matrix (ECM) signalling and vertebrate development, with some sessions being common to both meetings. Combining these two meetings has become increasingly appropriate given the emerging evidence for a fundamental role for the ECM and its receptors in embryonic development. This report gives an overview of the salient features of the ECM signalling portion of the meeting, which focused on cell–matrix and cell–cell interactions plus downstream signalling events.

**Integrins and their ECM ligands in proliferation, differentiation and cell-fate determination**

Integrins  $\alpha 5 \beta 1$  and  $\alpha v \beta 1$  are expressed by smooth muscle cells and

serve as important regulators of angiogenesis. Both fibronectin- and  $\alpha 5$ -integrin-null embryos die early during development, displaying defects in heart development and vasculogenesis<sup>1</sup>. Analysis of  $\alpha 5$ -null cells suggested that  $\alpha v \beta 1$  can substitute for  $\alpha 5 \beta 1$  and thus that the functions of  $\alpha v$  and  $\alpha 5$  might be similar<sup>2</sup>. To compare the knockout phenotypes of  $\alpha v$  and  $\alpha 5$ , Richard Hynes (Cambridge, USA) and colleagues generated mice lacking  $\alpha v$ . Eighty per cent of the  $\alpha v$ -null embryos died before birth, and the remaining 20% were born but died within one day with brain haemorrhages. Hynes proposed that vascularization in the brain, particularly, is dependent on the presence of a functional  $\alpha v$  integrin. Russell Ross (Seattle, USA) provided some molecular insight into

the function of integrins in angiogenesis. Ross showed that fibrillar collagen inhibits smooth muscle cell proliferation by suppressing cdk2 phosphorylation and upregulating the expression of the cyclin-dependent kinase (CDK) inhibitors p21 and p27. By contrast, monolayer collagen allows cells to induce cyclins A and E and proliferate in response to mitogens. Fibrillar collagen also inhibits the fibronectin receptors  $\alpha v \beta 1$  and  $\alpha 5 \beta 1$  and fibronectin fibril assembly, which is required for DNA synthesis in smooth muscle cells growing on monomeric collagen. Thus, integrin–matrix interactions appear to regulate smooth muscle cell proliferation positively or negatively depending on the microenvironment.

The overall theme of a given integrin transducing distinct signals depending on the composition of the ECM was a recurrent topic at the meeting. Fiona Watt (London, UK) discussed an important bidirectional role for integrins in cell-fate determination. During keratinocyte differentiation,  $\beta 1$  integrins can control the

\*Keystone Symposia on Extracellular Matrix Signalling and Vertebrate Development; Steamboat Springs, CO, USA; 3–8 April 1998. Organized by Zena Werb and Marc Tessier-Lavigne (ECM), Andrew P. McMahon and Douglas Melton (development).